

1 **Detection behavior of phenolic compounds in a dual-electrode system assembled**
2 **from track-etched membrane electrodes**

3

4 Tomohiko Kuwabara^a, Rikuo Hashimoto^a, Kenji Matsumoto^b, Hiroki Hotta^{b,c}, Masamitsu
5 Iiyama^d, Toshio Takayanagi^a, and Hitoshi Mizuguchi^{a*}

6

7 ^a Graduate School of Science and Technology, Tokushima University, 2-1 Minami-
8 Josanjima, Tokushima 770-8506, Japan

9 ^b Graduate School of Science, Technology and Innovation, Kobe University, 1-1
10 Rokkodai-cho, Nada-ku, Kobe, Hyogo, 657-8501, Japan

11 ^c Graduate School of Maritime Sciences, Kobe University, 5-1-1 Fukae-minamimachi,
12 Higashinada-ku, Kobe, Hyogo, 658-0022, Japan

13 ^d Nomura Micro Science Co., Ltd., 2-4-37, Okada, Atsugi, Kanagawa 243-0021, Japan

14

15 *Corresponding author. E-mail address: mizu@tokushima-u.ac.jp

16

17

18

19 **Abstract**

20 Electrochemical detection behavior of phenolic compounds in a series dual-electrode
21 detector constructed from track-etched membrane electrodes (TEMEs) was investigated
22 using microbore high-performance liquid chromatography. This detector featured
23 complete electrolysis provided by the electrode structure, which consisted of cylindrical
24 pores with a uniform diameter. The collection efficiency, which was defined as the ratio
25 of peak areas observed at the first and second working electrodes, ranged from negative
26 values up to 1.0. Because it reflected the electrochemical reaction's reversibility and the
27 reaction products' stability, the substance-inherent collection efficiency varied over a
28 much broader range of values than that obtained with conventional electrochemical
29 detectors. The collection efficiencies of catechol and hydroquinone were up to 1.0.
30 Resorcinol produced an anodic peak at both the first and second working electrodes
31 despite a lower potential for polarization of the second electrode than the first electrode.
32 In this case, the collection efficiency was negative. The results showed that the resulting
33 product was oxidized in a low potential region. Catechin compounds, which have both
34 catechol and resorcinol moieties, displayed the characteristics of both catechol and
35 resorcinol simultaneously. Gallic acid, which produced an irreversible cyclic
36 voltammogram, showed a quasi-reversible property produced by a relatively short

37 transition time in the dual-electrode detector. The reported data will be valuable for peak
38 identification and estimation of peak purities in complex chromatograms.

39

40 **Keywords:** Track-etched membrane filter, Dual-electrode detection, Complete
41 electrolysis, Collection efficiency, High-performance liquid chromatography–
42 electrochemical detection, Phenolic compound

43

44

45

46

47

48

49

50 **1. Introduction**

51 Improvement of separation-based analytical methods, such as high-performance
52 liquid chromatography (HPLC), has made it possible to focus on individual chemical
53 components in food, medicine, and biological samples. Among the available detection
54 methods, electrochemical detection is promising to investigate the role and dynamics of
55 trace materials because of the sensitivities and selectivities of certain substances that are
56 active in electrochemical reactions. This detection method has been applied to various
57 electrochemically active substances, such as phenolic compounds [1-5], phytochemicals
58 [6], pesticide residues [7,8], and vitamins [9,10]. As described in prominent review
59 articles [11-15], HPLC with electrochemical detection has been applied in a wide range
60 of analytical fields.

61 Dual-electrode systems are often used in electrochemical detection. This electrode
62 system, in which two closely located electrodes are arranged in series, parallel-adjacent,
63 or parallel-opposed positions, often has superior selectivity and sensitivity compared with
64 other electrode systems [11,13,14,16,17]. In a series dual-electrode system, oxidation and
65 reduction reactions proceed step-by-step at each electrode. Several operation modes, such
66 as screening mode, redox mode, and others, are available in this system. Screening mode
67 enables the removal of interfering species by oxidation or reduction at the upstream

68 working electrode. Redox mode allows for selective detection of substances with quasi-
69 reversible properties in electrochemical reactions. In this case, the collection efficiency,
70 which is defined as the ratio of the peak currents observed at the first and the second
71 electrodes, is the magnitude of the fraction of the first electrolysis product detected at the
72 second electrode. The collection efficiency reflects the reversibility in an electrochemical
73 reaction and the stability of the first electrolysis products, and can be helpful for peak
74 identification [18]. However, the collection efficiency also depends on the electrode
75 shape. For example, a disk-like electrode pair embedded in a thin layer flow cell used by
76 Roston et al. provided a limited collection efficiency of up to 37% [18]. Later, an
77 interdigitated microarray dual-electrode [19-21] and a split-disk dual-electrode [22] were
78 reported. These electrodes provided much higher collection efficiency and improved
79 detection limit based on redox cycling between two working electrodes.

80 We have previously proposed series multi-electrode systems using track-etched
81 membrane electrodes (TEMES) [23-27]. The electrode for these systems is prepared using
82 a track-etched membrane filter consisting of smooth flat surfaces and cylindrical pores
83 with a uniform diameter. The thickness of the membrane filter is approximately 10 μm .
84 This filter electrode provides highly efficient electrolysis of the electrolyte solution as it
85 filters through the electrode, and the efficiency is maintained close to 100% even at a

86 relatively high flow rate. Furthermore, the series multi-electrode system is easily
87 fabricated by alternately stacking the electrodes. Therefore, this configuration
88 simultaneously provides high electrolysis efficiency (~100%) and increased collection
89 efficiency (~100%) [23]. In previous studies, this electrode system was applied to flow
90 injection/anodic stripping voltammetry [24] and enzyme-based flow biosensors [25,26].
91 Microbore HPLC can be used for coulometric detection of catecholamines with an
92 improved flow cell, and redox-mode detection using a series dual-electrode detector is
93 also available [27].

94 In this study, we investigated the detection patterns of phenolic compounds in redox
95 mode using a series dual-electrode detection system incorporated into microbore HPLC
96 (Fig. 1). We expected that the collection efficiency available using this proposed flow cell
97 would be broader than that obtained in previous studies. The relationship between the
98 obtained values and the molecular structure is discussed. Furthermore, we found that
99 resorcinol and its analogues produced substances that were electrochemically oxidizable
100 in the region with a higher negative potential. These properties provide a wider variety of
101 collection efficiencies against individual materials than those given by traditional
102 electrochemical flow cell. The obtained data will be helpful for peak identification and
103 estimation of peak purity.

104

105 **2. Experimental**

106 *2.1. Reagents*

107 In this study, we investigated 11 types of phenolic compounds (Table 1) contained in
108 beverages of plant origins, such as coffee and tea. Catechol was purchased from Kanto
109 Chemical Co., Inc. (Tokyo, Japan). Hydroquinone, resorcinol, protocatechuic acid, and
110 pyrogallol were obtained from FUJIFILM Wako Pure Chemical Co. (Osaka, Japan).
111 Gentisic acid, caffeic acid, chlorogenic acid hydrate, gallic acid hydrate, and (+)-catechin
112 hydrate were purchased from Tokyo Chemical Industry Co., Ltd. (Tokyo, Japan). (-)-
113 Epicatechin was purchased from Combi-Blocks, Inc. (San Diego, CA). Standard solutions
114 of these compounds were prepared daily by dissolving them in water or acetonitrile
115 (HPLC grade, Kanto Chemical Co., Inc.). All other reagents were of the highest grade
116 available and were used without further purification. Deionized water (18 M Ω cm) was
117 generated using a water purification system (Milli-Q Gradient A10, Millipore).

118

119 *2.2. Electrochemical detector*

120 The structure of the electrochemical detector used in this study is shown in our
121 previous report [23,27]. Briefly, electrodes prepared using a track-etched microporous

122 membrane filter (pore size: 0.40 μm , porosity: 13%, thickness: 10 μm ; Whatman) were
123 arranged as the first and second working electrodes (WE1 and WE2, respectively), and
124 counter electrode along the eluent flow direction by alternately stacking the electrodes.
125 Track-etched membrane filters (pore size: 5.0 μm , thickness: 10 μm) were inserted
126 between the electrodes as spacers to prevent short circuits and keep a uniform distance
127 between the electrodes. A Ag/AgCl reference electrode (Model RE3V; ALS Co., Ltd.,
128 Tokyo, Japan) was placed 10 mm downstream of the counter electrode. A multi-channel
129 potentiostat (HA1010mM4A; Hokuto Denko Co., Tokyo, Japan) equipped with a
130 function generator (HB111A; Hokuto Denko Co.) was connected to each electrode for
131 the dual-electrode amperometric detection. A Chromato-PRO data processor (RunTime
132 Co., Hachioji, Japan) was used for data processing.

133

134 2.3. *Chromatography system*

135 The HPLC system consisted of an HPLC pump (LC20AD; Shimadzu Corp., Kyoto,
136 Japan) and an internal sample injector with a 0.2 μL injection volume (C4-1004-.2, Valco
137 Instruments Co., Inc., Houston, TX). The HPLC column was a Capillary EX InertSustain
138 C18 (50 mm \times 0.7 mm i.d., 3 μm particle size; GL Sciences Inc., Tokyo, Japan). The
139 chromatographic separation was carried out under isocratic conditions using an 8 % (w/v)

140 aqueous acetonitrile solution containing 0.1 M phosphoric acid and 0.1 M potassium
141 dihydrogen phosphate (pH 2.1 ± 0.1). The mobile phase flow rate was 0.05 mL min^{-1} .
142 Before each chromatography run, the eluent was treated by bubbling with argon for 30
143 min and ultrasonic degassing.

144

145 **3. Results and discussion**

146 *3.1. Detection behaviors of the phenolic compounds*

147 Typical chromatograms obtained using the proposed dual-electrode system are shown
148 in Fig. 2. In these chromatograms, positive peaks are anodic responses, and negative
149 peaks are cathodic responses. The potential of WE1 was adjusted to a value between +0.7
150 and +1.1 V. The cyclic voltammograms (CVs) showed that the electrochemical oxidation
151 of the phenolic compounds used in this study proceeded in this potential region (Fig. S1).
152 The chromatogram obtained when WE2 was polarized at -0.2 V is shown in Fig. S2. The
153 peak area is equivalent to the charge generated by the redox reaction on the electrodes
154 and is proportional to the number of electrons involved in the redox reaction and the
155 amount of electrolyzed substances by Coulomb's law as follows:

$$156 \quad C = nFcf_c \quad (1)$$

157 where C , n , F , c , V , and f_c are the peak area, the number of electrons involved in the redox

158 reaction, the Faraday constant (9.64846×10^4 C/equiv.), concentration, injection volume
159 (0.2 μ L), and electrolysis efficiency, respectively. The collection efficiency (N) was
160 defined as follows:

$$161 \quad N = -C_{WE2}/C_{WE1} \quad (2)$$

162 where C_{WE1} and C_{WE2} are the peak areas obtained at WE1 and WE2, respectively. The
163 anodic and cathodic peak areas can be positive and negative values. Equation 2 shows
164 that the collection efficiency is the ratio of electrolysis products from WE1 collected at
165 WE2, and it can vary from 0 to 1.0. However, the collection efficiency can be negative if
166 the substance has anodic peaks at both WE1 and WE2. The variations of C_{WE1} , C_{WE2} , and
167 N against the potential at WE1 are shown in Fig. 3. The anodic peaks derived from
168 substances such as catechol were accompanied by cathodic peaks and had positive
169 collection efficiencies (Fig. 4a and b). Especially when the applied potential at WE2 was
170 -0.2 V, the collection efficiencies of catechol and hydroquinone were up to 1.0 (Fig. 4a).
171 By contrast, the compounds such as resorcinol, catechin, and epicatechin had negative
172 collection efficiencies when the applied potential at WE1 was $+1.1$ V (Fig. 4d). The
173 collection efficiencies of pyrogallol and gallic acid were obtained from negative values
174 to 0.9 under the tested conditions in this study (Fig. 4b, c, and d). In the case of L-ascorbic
175 acid, the collection efficiency was 0, reflecting electrochemical irreversibility (Fig. 4c,

176 data not shown). These results indicate that the collection efficiency obtained with the
177 proposed detector varies over a broad range, and includes negative values. The collection
178 efficiency represents the stability and electrochemical properties of the electrolysis
179 product at WE1, and the collection efficiency observed under particular conditions is
180 closely related to the molecular structure. We classified the 11 phenolic compounds
181 according to their molecular structures to evaluate their detection behavior with the
182 proposed dual-electrode detector.

183

184 *3.2 Catechol and its analogues*

185 Catechol and its analogues, such as protocatechuic acid, caffeic acid, and chlorogenic
186 acid, which all contain the catechol moiety, produced an anodic peak at WE1 and a
187 corresponding cathodic peak at WE2 (Fig. 2B and C). In the case of catechol, the peak
188 area at WE1 (C_{WE1}) was larger in higher potential regions, and C_{WE1} reached a maximum
189 and constant value at potentials higher than +0.9 V (Fig. 3a). This value is close to the
190 total charge produced by the two-electron transfer reaction (1.93 μC). The collection
191 efficiency increased when the potential applied at WE2 was decreased, and reached 1.0
192 when WE2 was polarized at -0.2 V. It is well known that electrolysis of catechol in a
193 typical aqueous solution is accompanied by two-electron transfer [28,29]. The CVs

194 indicated a quasi-reversible property (see Fig. S1a, b, c, and d). Therefore, C_{WE1} and the
195 collection efficiency are controlled by the overpotentials for catechol oxidation and
196 reduction of its anodic product, respectively. A sufficiently large overpotential provides
197 complete electrolysis in these reactions.

198 In the case of protocatechuic acid, caffeic acid, and chlorogenic acid, which contain
199 side-chains linked to the aromatic ring, the peak area (C_{WE1}) increased at higher potential
200 but complete electrolysis was not achieved. The maximum collection efficiencies were
201 obtained at +1.0 V. Although the collection efficiency tended to be higher when the
202 potential at WE2 was lower, the values were less than 0.9 under the conditions tested in
203 this study (Fig. 3b, c, and d). In this case, the detection type was as shown in Fig. 4b. The
204 CVs showed the oxidation potential of protocatechuic acid was slightly higher than that
205 of catechol, whereas those of caffeic acid and chlorogenic acid were almost the same as
206 that of catechol. Despite the similar electrochemical properties, the electrolysis
207 efficiencies and collection efficiencies of these substances were lower than that of
208 catechol. The efficiency of electrolysis is also affected by the flow rates. In another
209 experiment under the different flow rate ranging from $0.025 \text{ mL min}^{-1}$ to $0.075 \text{ mL min}^{-1}$,
210 both the electrolysis efficiency and collection efficiency of chlorogenic acid slightly
211 increased as flow rates decreased (data not shown). These phenomena including the

212 difference in electrolysis efficiencies may be caused by the electron-withdrawing
213 inductive effect of the carboxyl group [30] and dimerization side reactions.
214 Electrochemical oxidation of caffeic acid and chlorogenic acid is known to be
215 accompanied by subsequent chemical reactions such as hydroxylation or dimerization
216 [31-35], and our results are consistent with these facts.

217

218 *3.3 Hydroquinone and gentisic acid*

219 The chromatograms obtained for hydroquinone and gentisic acid, an analogue of
220 hydroquinone, are shown in Fig. 2A and Fig. S2A. The peak areas (C_{WE1}) for these
221 substances increased at higher potentials. The values of C_{WE1} reached a maximum and
222 constant value close to the total charge produced by the two-electron transfer reaction
223 (1.93 μC). When WE2 was polarized at -0.2 V, anodic peaks and corresponding cathodic
224 peaks were observed at WE1 and WE2, respectively (Fig. 3e). Gentisic acid produced
225 anodic and cathodic peaks even when WE2 was polarized at $+0.2$ V. The collection
226 efficiencies increased when the applied potential at WE2 decreased, and reached 1.0 over
227 in a wider potential range than that was the case for catechol (Fig. 3f). The CVs indicated
228 hydroquinone had a quasi-reversible property, and the redox reaction of gentisic acid was
229 accompanied by side reactions (see Fig. S1e and f). In the case of hydroquinone, the

230 detection behavior can be explained by the overpotentials for the electrochemical
231 oxidation of hydroquinone and the reduction of its anodic products. However, a small
232 anodic response appeared at WE2 when WE2 was polarized at +0.2 V. This anode peak
233 at WE2 became slightly more significant when the applied potential of WE2 was set at
234 +0.3 or +0.4 V (data not shown). The detail of this phenomenon remains to be investigated.
235 But the anodic product at WE1 may have been oxidized at WE2, which is polarized at
236 lower potentials. The transition time from WE1 to WE2 is expected to be 7.4 μ s, assuming
237 that radial dispersion in the proposed flow cell never occurs [27]. Therefore, the distinct
238 cathodic peaks at WE2 of gentisic acid clearly arise because of the rapid transfer of the
239 anodic product to WE2 before the side reactions progress.

240

241 *3.4 Resorcinol*

242 The chromatograms produced by resorcinol are shown in Fig. 2A and Fig. S2A. The
243 peak areas (C_{WE1}) increased in the higher potential region (Fig. 3g). In contrast to catechol
244 and hydroquinone, resorcinol produced a distinct anodic peak at WE2 when the applied
245 potential at WE1 was +1.1 V. In this case, the detection type was as shown in Fig. 4d.
246 The intensity of this anodic peak at WE2 was much greater than that observed at WE1,
247 which was polarized at +0.2 V. This result clearly shows that the electrochemical

248 oxidation product at WE1 is further oxidized at WE2, producing the anodic peak at WE2.
249 The CV was irreversible for the electrochemical reaction of resorcinol, with gradual decay
250 of the anodic peak observed with repeated potential cycles (see Fig. S1g). The
251 electrochemical oxidation of resorcinol is known to form a dimer or polymer on the
252 electrode surface, which is accompanied by a loss of electrode activity [36-38]. We have
253 previously reported that one of the products produced by oxidation of resorcinol by the
254 ABTS radical is more readily oxidized than the original resorcinol [39]. Our results
255 indicate that the anodic product of resorcinol at WE1 is oxidized at WE2, which is
256 polarized at a lower potential than at WE1. This is consistent with the results reported in
257 the previous study. Although the mechanism of the reactions in the proposed detector still
258 needs to be investigated in detail, we found that resorcinol gives both anodic peaks,
259 providing negative collection efficiency. Because the electrolysis product at WE1 moves
260 quickly to WE2, this dual electrode detector readily provides the unique characteristics
261 of resorcinol that distinguish it from other phenolic compounds.

262

263 *3.5 Catechin compounds*

264 The chromatograms produced by catechin and epicatechin are shown in Fig. 2D and
265 Fig. S2E. The peak areas (C_{WE1}) for these substances increased gradually in the higher

266 potential region and reached maxima of 3.26 and 3.98 μC for catechin and epicatechin,
267 respectively, at +1.0 V (Fig. 3h and i). These values are much larger than those obtained
268 for the two-electron reaction. Small anodic peaks were obtained at WE2 with polarization
269 at +0.2 V, whereas cathodic peaks were obtained when the applied potential was -0.2 V.
270 When the applied potential at WE1 was +1.1 V, anodic peaks were obtained at WE2, and
271 these gave negative collection efficiencies. The CVs of catechin and epicatechin are
272 shown in Fig. S1h and i. Irreversible properties with two anodic peaks were observed
273 with a gradual decrease in the current observed with repeated sweeping of the potential
274 between 0 and +1.0 V. When the scan range was between 0 and +0.75 V, quasi-reversible
275 CVs were obtained. Catechin compounds contain catechol and resorcinol moieties, which
276 can undergo electrochemical oxidation [40-42]. Comparison of the CVs suggests that the
277 quasi-reversible property originates from the catechol moiety, and the irreversible
278 property is derived from electrochemical oxidation of the resorcinol moiety and
279 subsequent side reactions. Therefore, catechin compounds displayed the characteristics
280 of both catechol and resorcinol simultaneously in the proposed detector system. The
281 relatively high collection efficiencies (0.1–0.6) obtained in the lower potential range of
282 WE1 from +0.7 to +1.0 V reflect the electrochemical quasi-reversibility of the catechol
283 moiety. In this case, these compounds indicate the detection type of Fig. 4b. By contrast,

284 the negative collection efficiency obtained at the higher potential of +1.1 V reflects the
285 irreversible property of the resorcinol moiety. Under this potential condition, the dual-
286 electrode detector provides the detection type shown in Fig. 4d for the catechin
287 compounds.

288

289 *3.6 Pyrogallol analogue*

290 The chromatograms obtained for pyrogallol and gallic acid are shown in Fig. 2C and
291 D, and Fig. S2C and D. In the case of pyrogallol, C_{WE1} increased at higher potentials and
292 reached a maximum of 3.47 μC at potentials higher than +0.9 V (Fig. 3j). This value was
293 higher than that obtained with the three-electron reaction. The cathodic peak was obtained
294 at WE2 with 0 or -0.2 V applied, and the peak area gradually decreased as the WE1
295 potential increased. By contrast, an anodic peak was observed when WE2 was polarized
296 at +0.2 V, and the collection efficiency became negative. Additionally, the peak area
297 (C_{WE2}) slightly increased when the potential applied at WE1 was +1.1 V. This result
298 indicates that the anodic product of pyrogallol at WE1 is easier to oxidize than pyrogallol.
299 In the case of gallic acid, the peak area (C_{WE1}) increased in the higher potential region,
300 but was much smaller than that of pyrogallol (Fig. 3k). The second electrode, WE2,
301 produced cathodic peaks under the conditions tested in this study. The conventional CVs

302 of pyrogallol and gallic acid showed irreversible properties with two anodic peaks (Fig.
303 S1j and k). The two peaks arose from two-step electrochemical oxidation of the pyrogallol
304 moiety via a quinone radical [38,43,44]. Hamid et al. reported that gallic acid displayed
305 a quasi-reversible CV with a fast potential sweep using a modified glassy carbon electrode
306 [44]. This indicates that the anodic products are relatively unstable but electrochemically
307 reducible. Therefore, our results with cathodic peaks at WE2 can be explained by the
308 quick transfer from WE1 to WE2 in a short time in the proposed detector. The difference
309 in the detection behavior between pyrogallol and gallic acid may be caused by the
310 electron-withdrawing inductive effect of the carboxyl group [30]. Although further
311 investigations are needed to clarify the detailed mechanism of the reactions, the proposed
312 dual-electrode detector provides unique values for the collection efficiency of each
313 substance.

314

315 *3.7 Application to an actual sample*

316 To clarify the applicability of the proposed method to actual samples, we conducted
317 the detection of phenolic compounds in a coffee drink. In this study, we used a retail-
318 released coffee drink from the market. The drink sample was diluted 10 times after
319 filtration, and then injected into the HPLC system. The obtained chromatogram is shown

320 in Fig. S3. Major components in the coffee sample provided anodic peaks at WE1 and
321 corresponding peaks at WE2. This result indicates that the coffee drink contains a lot of
322 substances having reversibility in the electrochemical reaction. From the retention time
323 and the detection behaviors, the peaks (a) and (b) in Fig. S3 were assigned to chlorogenic
324 acid and caffeic acid, respectively. Fig. S4 shows the calibration plots. The detection
325 limits of these compounds were both $0.7 \mu\text{M}$. The concentration of chlorogenic acid and
326 caffeic acid in the diluted coffee sample were $16.6 \pm 0.9 \mu\text{M}$ and $3.6 \pm 0.2 \mu\text{M}$, respectively.
327 The collection efficiencies of chlorogenic acid and caffeic acid contained in the coffee
328 drink sample were 0.85 ± 0.01 and 0.85 ± 0.14 , respectively. These values were close to
329 those obtained by the standard solution (0.82 ± 0.18 for chlorogenic acid and 0.84 ± 0.08
330 for caffeic acid). Therefore, the purities of these peaks were relatively high, and both
331 chlorogenic acid and caffeic acid were separated enough from other components. Suppose
332 there is a significant difference in the collection efficiencies between actual and standard
333 samples despite the same retention time. In that case, there is a possibility that the peaks
334 of other components are overlapped. As described above, the method described herein
335 can provide useful peak identification feature for the phenolic compounds.

336

337 **4. Conclusions**

338 In this study, we investigated the detection behaviors of 11 types of phenolic
339 compounds in a dual-electrode detector that was constructed using TEMEs. The
340 relationship between the molecular structure and detection behavior was evaluated. The
341 collection efficiencies of phenolic compounds covered a broad range from negative
342 values to 1.0, which reflected their molecular structures and electrochemical properties.
343 Catechol, hydroquinone, and their analogues had high collection efficiencies (up to 1.0),
344 which reflected the reversibility of the electrochemical reactions. By contrast, resorcinol
345 produced anodic peaks at both WE1 and WE2, and the collection efficiency was negative.
346 Catechin provided a wide range of collection efficiencies depending on the detection
347 conditions. When the applied potential at the first electrode was below +1.0 V, the
348 collection efficiency ranged from 0 to 0.6, which corresponded to a quasi-reversible
349 property originating from the catechol moiety. By contrast, a negative collection
350 efficiency originating from the properties of resorcinol moiety was obtained when the
351 potential applied at WE1 was +1.1 V. Pyrogallol and gallic acid gave positive collection
352 efficiencies ranging from 0 to 0.7 despite having irreversible CVs. These results indicate
353 that the detection behavior observed in the proposed dual-electrode detector is
354 characterized by the electrochemical reversibility and rate of the subsequent chemical
355 reaction, and gives substance-inherent values under specific conditions. Therefore, the

356 chromatograms obtained by the proposed detector contain helpful information for peak
357 identification and peak purity. We believe the data reported herein will be beneficial for
358 qualitative and quantitative detection of target analytes in food, medicine, and biological
359 samples with complex matrices.

360

361 **ORCID**

362 Hitoshi Mizuguchi: 0000-0003-2396-6812

363 Toshio Takayanagi: 0000-0002-5767-1126

364 Hiroki Hotta: 0000-0002-1637-5849

365

366 **Author contributions**

367 Tomohiko Kuwabara: Conceptualization, Methodology, Investigation, Visualization,
368 Writing-Original draft, Funding acquisition. Rikuo Hashimoto: Investigation,
369 Visualization. Kenji Matsumoto: Methodology, Writing – Review & Editing. Hiroki
370 Hotta: Methodology, Writing – Review & Editing. Masamitsu Iiyama: Methodology,
371 Funding acquisition. Toshio Takayanagi: Methodology. Hitoshi Mizuguchi: Supervision,
372 Conceptualization, Methodology, Investigation, Visualization, Writing – Review &
373 Editing, Funding acquisition.

374

375 **Conflict of interest**

376 H.M. and M.I. have a patent pending to JP, 2020-012722, A. This work was partially

377 funded by Nomura Micro Science Co. Ltd., to which one of the authors (M.I.) belongs.

378 The sponsor had no control over this work's interpretation, writing, or publication.

379

380 **Acknowledgements**

381 This work was supported by Japan Society for the Promotion of Science (JSPS)

382 KAKENHI (Grant Number JP 21K19869). The authors thank Mr. Noboru Imoto (a

383 technical staff member of Yamagata University) for helpful assistance in construction of

384 the flow cell. We thank Gabrielle David, PhD, from Edanz (<https://jp.edanz.com/ac>) for

385 editing a draft of this manuscript.

386

387 **Supplementary data**

388 Supplementary data for this article can be found online at <https://>

389

390

391 **References**

392 [1] P. Jandera, V. Škeříková, L. Řehová, T. Hájek, L. Baldriánová, G. Škopová, V.
393 Kellner, A. Horna, RP-HPLC analysis of phenolic compounds and flavonoids in
394 beverages and plant extracts using a CoulArray detector, *J. Sep. Sci.*, **28** (2005)
395 1005–1022.

396 <https://doi.org/10.1002/jssc.200500003>

397 [2] A. M. Danila, A. Kotani, H. Hakamata, F. Kusu, Determination of rutin, catechin,
398 epicatechin, and epicatechin gallate in buckwheat *fagopyrum esculentum moench* by
399 micro-high-performance liquid chromatography with electrochemical detection, *J. Agric.*
400 *Food Chem.*, **55** (2007) 1139–1143.

401 <https://doi.org/10.1021/jf062815i>

402 [3] P. V. Freitas, D. R. da Silva, M. A. Beluomini, J. L. da Silva, N. R. Stradiotto,
403 Determination of phenolic acids in sugarcane vinasse by HPLC with pulse amperometry,
404 *J. Anal. Methods Chem.*, **2018** (2018) 1–10.

405 <https://doi.org/10.1155/2018/4869487>

406 [4] C. Bocchi, M. Careri, F. Groppi, A. Mangia, P. Manini, G. Mori, Comparative
407 investigation of UV, electrochemical and particle beam mass spectrometric detection for
408 the high-performance liquid chromatographic determination of benzoic and cinnamic
409 acids and of their corresponding phenolic acids, *J. Chromatogr. A*, **753** (1996) 157–170.

410 [https://doi.org/10.1016/S0021-9673\(96\)00561-4](https://doi.org/10.1016/S0021-9673(96)00561-4)

411 [5] M. Akasbi, D. W. Shoeman, A. Saari Csallany, High-performance liquid
412 chromatography of selected phenolic compounds in olive oils, *JAOCS*, **70** (1993)
413 367–370.

414 <https://doi.org/10.1007/BF02552708>

415 [6] C. R. Correa, L. Li, G. Aldini, M. Carini, C. Y. Oliver Chen, H. K. Chun, S. M. Cho,
416 K. M. Park, R. M. Russell, J. B. Blumberg, K. J. Yeum, Composition and stability of
417 phytochemicals in five varieties of black soybeans (*Glycine max*), *Food Chem.*, **123**
418 (2010) 1176–1184.

419 <https://doi.org/10.1016/j.foodchem.2010.05.083>

420 [7] C. F. B. Coutinho, L. F. M. Coutinho, L. H. Mazo, S. L. Nixdorf, C. A. P. Camara,
421 Rapid and direct determination of glyphosate and aminomethylphosphonic acid in water
422 using anion-exchange chromatography with coulometric detection, *J. Chromatogr. A*,
423 **1208** (2008) 246–249.

424 <https://doi.org/10.1016/j.chroma.2008.09.009>

425 [8] R. Wintersteiger, B. Goger, H. Krautgartner, Quantitation of chlorophenoxy acid
426 herbicides by high-performance liquid chromatography with coulometric detection, *J.*
427 *Chromatogr. A*, **846** (1999) 349–357.

428 [https://doi.org/10.1016/S0021-9673\(99\)00429-X](https://doi.org/10.1016/S0021-9673(99)00429-X)

429 [9] H. Iwase, Routine high-performance liquid chromatographic determination of
430 ascorbic acid in foods using L-methionine for the pre-analysis sample stabilization,
431 *Talanta*, **60** (2003) 1011–1021.

432 [https://doi.org/10.1016/S0039-9140\(03\)00180-2](https://doi.org/10.1016/S0039-9140(03)00180-2)

433 [10] A. Lebidzińska, M. L. Marszałł, J. Kuta, P. Szefer, Reversed-phase high-
434 performance liquid chromatography method with coulometric electrochemical and
435 ultraviolet detection for the quantification of vitamins B₁ (thiamine), B₆ (pyridoxamine,
436 pyridoxal and pyridoxine) and B₁₂ in animal and plant foods, *J. Chromatogr. A*, **1173**
437 (2007) 71–80.

438 <https://doi.org/10.1016/j.chroma.2007.09.072>

439 [11] M.C. Santamaría, M. M. Barambio, A. S. Arribas, HPLC techniques with
440 electrochemical detection, in: A. Escarpa, M. C. González, M. Á. Lopez (Eds.),
441 *Agricultural and Food Electroanalysis*, Wiley, 2015, pp. 73–116.

442 <https://doi.org/10.1002/9781118684030.ch1>

443 [12] R. J. Flanagan, D. Perrett, R. Whelpton (Eds.), *Electrochemical Detection in HPLC:*
444 *Analysis of Drugs and Poisons*, Royal society of Chemistry, London, 2005.

445 <https://doi.org/10.1039/9781847550729>

- 446 [13] G. Sontag, M. I. Pinto, J. P. Noronha, H. D. Burrows, Analysis of food by high
447 performance liquid chromatography coupled with coulometric detection and related
448 techniques: a review, *J. Agric. Food Chem.*, **67** (2019) 4113–4144.
449 <https://doi.org/10.1021/acs.jafc.9b00003>
- 450 [14] K. C. Honeychurch, Design and application of liquid chromatography dual electrode
451 detection, in: C. Banks, R. Mortimer, S. McIntosh (Eds.), *Electrochemistry*, vol. 13, Royal
452 Society of Chemistry, 2016, pp. 1–20.
453 <https://doi.org/10.1039/9781782620273-00001>
- 454 [15] H. Hotta, K. Matsumoto, Evaluation of antioxidant activity by flow injection analysis
455 with electrochemical detection, *J. Flow Inj. Anal.*, **35** (2018) 49–51.
456 https://doi.org/10.24688/jfia.35.2_49
- 457 [16] C. L. Blank, Dual electrochemical detector for liquid chromatography, *J. Chromatogr.*
458 *A*, **117** (1976) 35–46.
459 [https://doi.org/10.1016/S0021-9673\(00\)81063-8](https://doi.org/10.1016/S0021-9673(00)81063-8)
- 460 [17] C. E. Lunte, P. T. Kissinger, R. E. Shoup, Difference mode detection with thin-layer
461 dual electrode liquid chromatography/electrochemistry, *Anal. Chem.*, **57** (1985)
462 1541–1546.
463 <https://doi.org/10.1021/ac00285a011>

464 [18] D. A. Roston, P. T. Kissinger, Series dual-electrode detector for liquid
465 chromatography/electrochemistry, *Anal. Chem.*, **54** (1982) 429–434.
466 <https://doi.org/10.1021/ac00240a019>

467 [19] O. Niwa, H. Tabei, B. P. Solomon, F. Xie, P. T. Kissinger, Improved detection limit
468 for catecholamines using liquid chromatography-electrochemistry with a carbon
469 interdigitated array microelectrode, *J. Chromatogr. B*, **670** (1995) 21-28.
470 [https://doi.org/10.1016/0378-4347\(95\)00145-9](https://doi.org/10.1016/0378-4347(95)00145-9)

471 [20] A. Aoki, T. Matsue, I. Uchida, Electrochemical response at microarray electrodes in
472 flowing streams and determination of catecholamines, *Anal. Chem.*, **62** (1990) 2206-2210.
473 <https://doi.org/10.1021/ac00219a010>

474 [21] H. Tabei, M. Takahashi, S. Hoshino, O. Niwa, T. Horiuchi, Subfemtomole detection
475 of catecholamine with interdigitated array carbon microelectrodes in HPLC, *Anal. Chem.*,
476 **66** (1994) 3500-3502.
477 <https://doi.org/10.1021/ac00092a031>

478 [22] O. Niwa, M. Morita, B.P. Solomon, P.T. Kissinger, Carbon film based ring-disk and
479 split-disk dual electrodes as detectors for microbore liquid chromatography,
480 *Electroanalysis*, **8** (1996) 427-433.
481 <https://doi.org/10.1002/elan.1140080505>

- 482 [23] H. Mizuguchi, K. Shibuya, A. Fuse, T. Hamada, M. Iiyama, K. Tachibana, T. Nishina,
483 J. Shida, A dual-electrode flow sensor fabricated using track-etched microporous
484 membranes, *Talanta*, **96** (2012) 168–173.
485 <https://doi.org/10.1016/j.talanta.2012.02.001>
- 486 [24] H. Mizuguchi, K. Numata, C. Monma, M. Iiyama, K. Tachibana, T. Nishina, J. Shida,
487 Determination of ultra-trace mercury(II) by flow-injection/anodic stripping voltammetry
488 using a track-etched microporous membrane electrode, *Anal. Sci.*, **29** (2013) 949–954.
489 <https://doi.org/10.2116/analsci.29.949>
- 490 [25] H. Mizuguchi, J. Sakurai, Y. Kinoshita, M. Iiyama, T. Kijima, K. Tachibana, T.
491 Nishina, J. Shida, Flow-based biosensing system for glucose fabricated by using track-
492 etched microporous membrane electrodes, *Chem. Lett.*, **42** (2013) 1317–1319.
493 <https://doi.org/10.1246/cl.130594>
- 494 [26] H. Mizuguchi, K. Sasaki, H. Ichinose, S. Seino, J. Sakurai, M. Iiyama, T. Kijima, K.
495 Tachibana, T. Nishina, T. Takayanagi, J. Shida, A triple-electrode based dual-biosensor
496 system utilizing track-etched microporous membrane electrodes for the simultaneous
497 determination of L-lactate and D-glucose, *Bull. Chem. Soc. Jpn.*, **90** (2017) 1211–1216.
498 <https://doi.org/10.1246/bcsj.20170193>
- 499 [27] H. Mizuguchi, D. Nishimori, T. Kuwabara, M. Takeuchi, M. Iiyama, T. Takayanagi,

500 Track-etched membrane-based dual-electrode coulometric detector for
501 microbore/capillary high-performance liquid chromatography, *Anal. Chim. Acta*, **1102**
502 (2020) 46–52.
503 <https://doi.org/10.1016/j.aca.2019.12.045>

504 [28] Q. Lin, Q. Li, C. Batchelor-McAuley, R. G. Compton, Two-electron, two-proton
505 oxidation of catechol: kinetics and apparent catalysis, *J. Phys. Chem. C*, **119** (2015)
506 1489–1495.
507 <https://doi.org/10.1021/jp511414b>

508 [29] A. J. Saleh Ahammad, S. Sarker, M. Aminur Rahman, J. J. Lee, Simultaneous
509 determination of hydroquinone and catechol at an activated glassy carbon electrode,
510 *Electroanalysis*, **22** (2010) 694–700.
511 <https://doi.org/10.1002/elan.200900449>

512 [30] B. Nasr, T. Hsen, G. Abdellatif, Electrochemical treatment of aqueous wastes
513 containing pyrogallol by BDD-anodic oxidation, *J. Environ. Manage.*, **90** (2009) 523–530.
514 <https://doi.org/10.1016/j.jenvman.2007.12.007>

515 [31] M. Namazian, H. R. Zare, Electrochemistry of chlorogenic acid: experimental and
516 theoretical studies, *Electrochim. Acta*, **50** (2005) 4350–4355.
517 <https://doi.org/10.1016/j.electacta.2005.01.043>

518 [32] H. Hotta, H. Sakamoto, S. Nagano, T. Osakai, Y. Tsujino, Unusually large numbers
519 of electrons for the oxidation of polyphenolic antioxidants, *Biochim. Biophys. Acta*, **1526**
520 (2001) 159–167.

521 [https://doi.org/10.1016/S0304-4165\(01\)00123-4](https://doi.org/10.1016/S0304-4165(01)00123-4)

522 [33] H. Hotta, S. Nagano, M. Ueda, Y. Tsujino, J. Koyama, T. Osakai, Higher radical
523 scavenging activities of polyphenolic antioxidants can be ascribed to chemical reactions
524 following their oxidation, *Biochim. Biophys. Acta*, **1572** (2002) 123–132.

525 [https://doi.org/10.1016/S0304-4165\(02\)00285-4](https://doi.org/10.1016/S0304-4165(02)00285-4)

526 [34] H. Hotta, M. Ueda, S. Nagano, Y. Tsujino, J. Koyama, T. Osakai, Mechanistic study
527 of the oxidation of caffeic acid by digital simulation of cyclic voltammograms, *Anal.*
528 *Biochem.*, **303** (2002) 66–72.

529 <https://doi.org/10.1006/abio.2002.5577>

530 [35] R. Arakawa, M. Yamaguchi, H. Hotta, T. Osakai, T. Kimoto, Product analysis of
531 caffeic acid oxidation by on-line electrochemistry/electrospray ionization mass
532 spectrometry, *J. Am. Soc. Mass Spectromet.*, **15** (2004) 1228–1236.

533 <https://doi.org/10.1016/j.jasms.2004.05.007>

534 [36] A. R. L. d. Silva, A. J. d. Santos, C. A. Martínez-Huitle, Electrochemical
535 measurements and theoretical studies for understanding the behavior of catechol,

536 resorcinol and hydroquinone on the boron doped diamond surface, RSC Adv., **8** (2018)
537 3483–3492.
538 <https://doi.org/10.1039/C7RA12257H>

539 [37] K. Kaewket, S. Maensiri, K. Ngamchuea, Adsorptive stripping voltammetry at
540 microporous carbon: Determination and adsorption characteristics of environmental
541 contaminants, Colloids Interface Sci. Commun., **38** (2020) 100310.
542 <https://doi.org/10.1016/j.colcom.2020.100310>

543 [38] H. Nady, M. M. El-Rabiei, G. M. A. El-Hafez, Electrochemical oxidation behavior
544 of some hazardous phenolic compounds in acidic solution, Egypt. J. Pet., **26** (2017)
545 669–678.
546 <https://doi.org/10.1016/j.ejpe.2016.10.009>

547 [39] K. Matsumoto, M. Taniarashi, Y. Tsutaho, A. Yamada, A. Yosho, T. Osakai, H.
548 Hotta, Redox reactions between ABTS•+ and dihydroxybenzenes as studied by cyclic
549 voltammetry, Anal. Sci., **38** (2022) 227–230.
550 <https://doi.org/10.2116/analsci.21N030>

551 [40] H. Muguruma, S. Murakami, S. Takahashi, N. Osakabe, H. Inoue, T. Ohsawa,
552 Separationless and adsorptionless quantification of individual catechins in green tea with
553 a carbon nanotube-carboxymethylcellulose electrode, J. Agric. Food Chem., **67** (2019)

554 943–954.

555 <https://doi.org/10.1021/acs.jafc.8b05540>

556 [41] P. Janeiro, A. M. O. Brett, Catechin electrochemical oxidation mechanisms, *Anal.*
557 *Chim. Acta*, **518** (2004) 109–115.

558 <https://doi.org/10.1016/j.aca.2004.05.038>

559 [42] K. Matsuura, Y. Usui, T. Kan, T. Ishii, T. Nakayama, Structural specificity of electric
560 potentials in the coulometric-array analysis of catechins and theaflavins, *J. Clin. Biochem.*
561 *Nutr.*, **55** (2014) 103–109.

562 <https://doi.org/10.3164/jcbtn.13-101>

563 [43] R. A. Hamid, E. F. Newair, Electrochemical behavior of antioxidants: I. Mechanistic
564 study on electrochemical oxidation of gallic acid in aqueous solutions at glassy-carbon
565 electrode, *J. Electroanal. Chem.*, **657** (2011) 107–112.

566 <https://doi.org/10.1016/j.jelechem.2011.03.030>

567 [44] R. A. Hamid, E. F. Newair, Adsorptive stripping voltammetric determination of
568 gallic acid using an electrochemical sensor based on polyepinephrine/glassy carbon
569 electrode and its determination in black tea sample, *J. Electroanal. Chem.*, **704** (2013)
570 32–37.

571 <https://doi.org/10.1016/j.jelechem.2013.06.006>

572 **Figures**

573

574

575

576

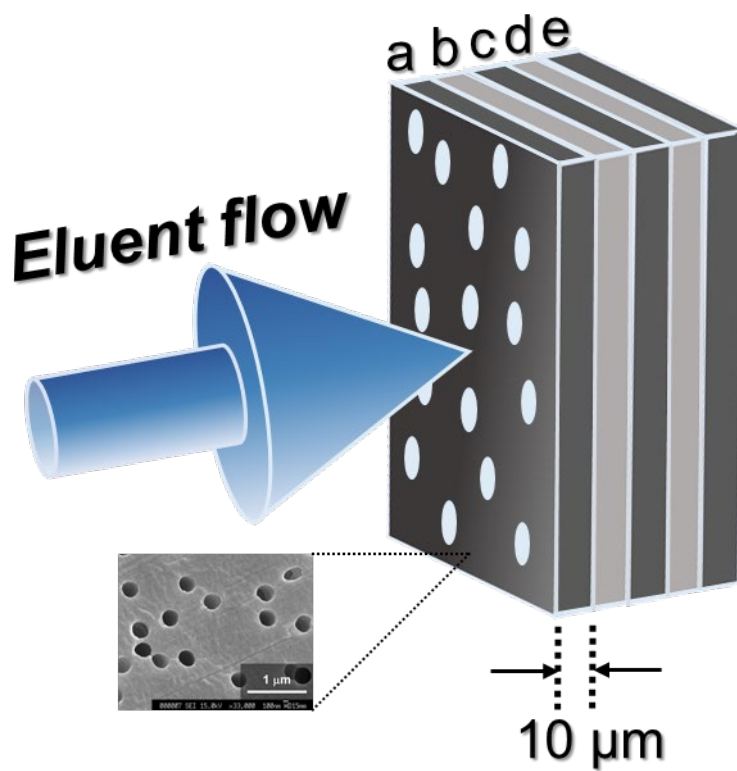
577

578

579

580

581



582 **Fig. 1.** Schematic representation of the series HPLC dual-electrode detection system

583 constructed with TEMEs. a: The first working electrode (WE1), b, d: spacers, c: the

584 second working electrode (WE2), e: counter electrode. The structure of electrochemical

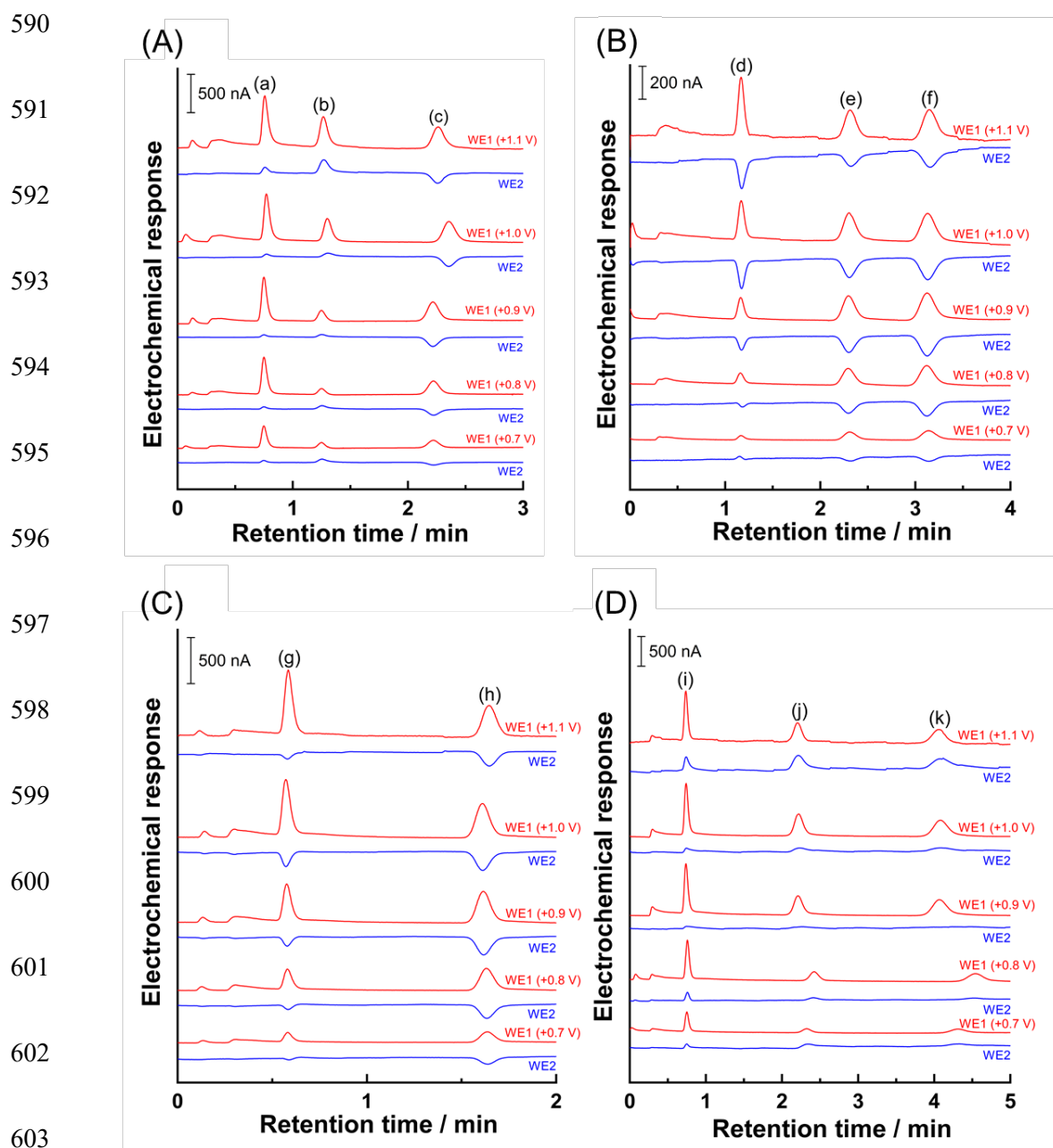
585 flow cell has been shown literature for detail [27].

586

587

588

589



590
 591
 592
 593
 594
 595
 596
 597
 598
 599
 600
 601
 602
 603
 604 **Fig. 2.** A typical chromatogram obtained by injecting a sample containing phenolic
 605 compounds. The sample solution for A was the mixture of hydroquinone (a), resorcinol
 606 (b), and gentisic acid (c). The sample solution for B had protocatechuic acid (d),
 607 chlorogenic acid (e), and caffeic acid (f). The sample solution for C contained gallic acid

608 (g) and catechol (h). The sample solution for D had pyrogallol (i), catechin (j), and
609 epicatechin (k). The concentration of each phenolic compound was 50 μM . The applied
610 potential at WE2 was +0.2 V.

611

612

613

614

615

616

617

618

619

620

621

622

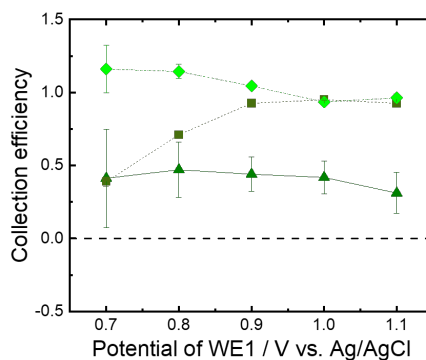
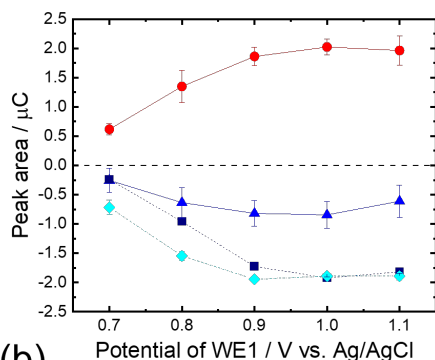
623

624

625

626

(a)



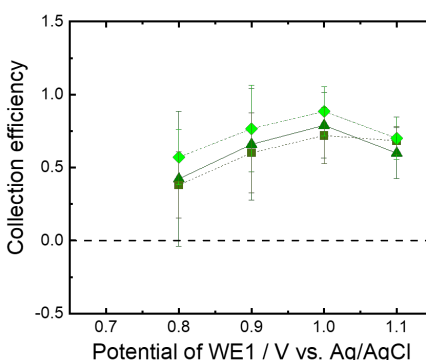
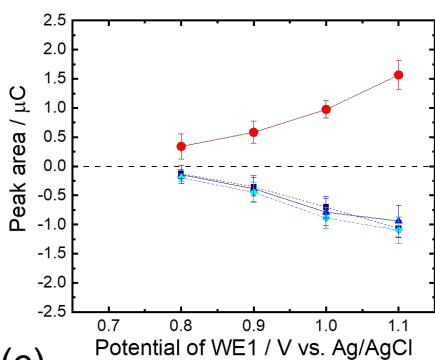
627

628

629

630

(b)



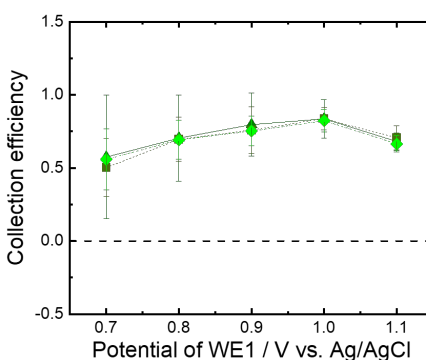
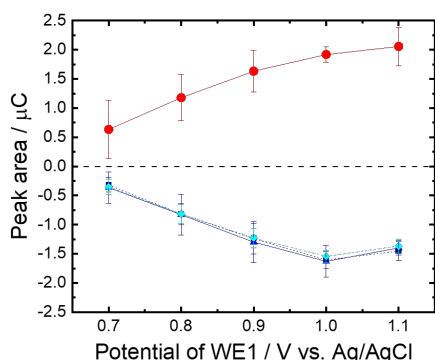
631

632

633

634

(c)



635

636

637

638

639 **Fig. 3.** The relationship between the potential applied at the first working electrode (WE1)

640 and the peak area at WE1 (C_{WE1} , closed circle), peak area at the second working electrode

641 (C_{WE2}), or the collection efficiency (N) obtained by analysis of chromatograms of catechol

642 (a), protocatechuic acid (b), caffeic acid (c), chlorogenic acid (d), hydroquinone (e),

643 gentisic acid (f), resorcinol (g), catechin (h), epicatechin (i), pyrogallol (j), and gallic acid

644 (k). The applied potential at WE1 was adjusted between +0.7 V and +1.1 V, and the
645 applied potential at WE2 was +0.2 V (closed triangle), 0.0 V (closed square), and -0.2 V
646 (closed rhombus), respectively.

647

648

649

650

651

652

653

654

655

656

657

658

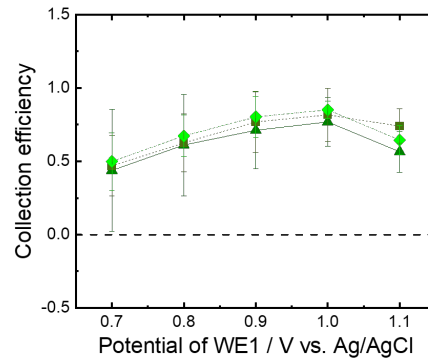
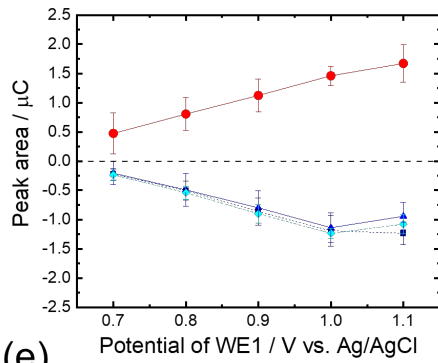
659

660

661

662

(d)



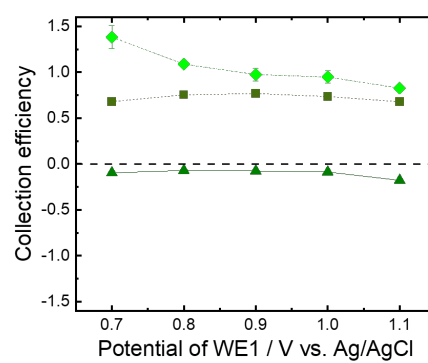
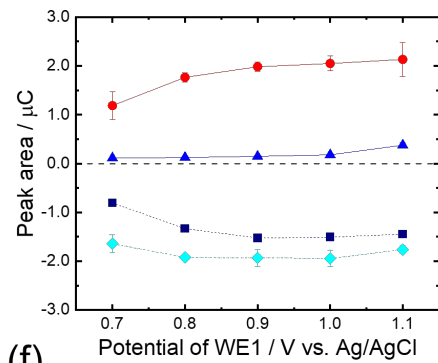
663

664

665

666

(e)



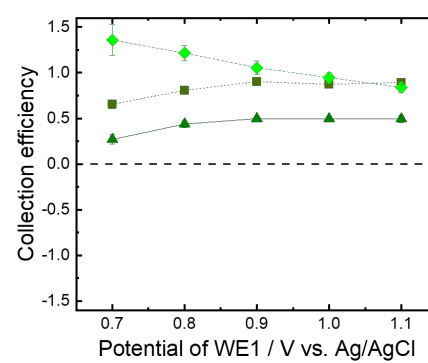
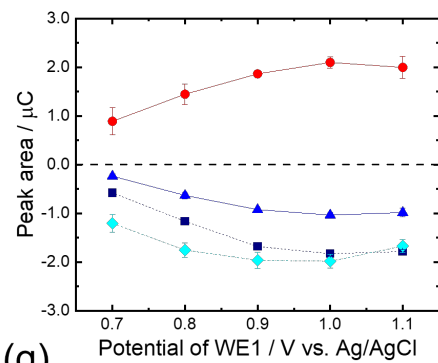
667

668

669

670

(f)



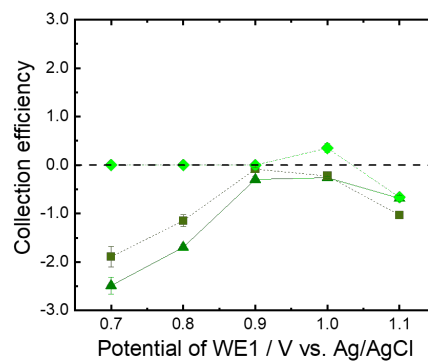
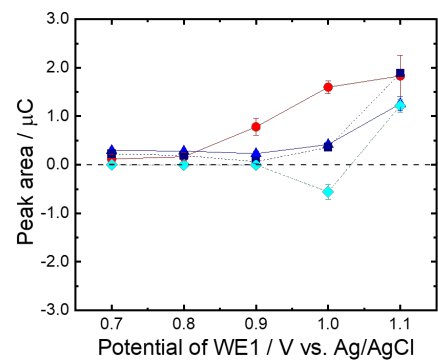
671

672

673

674

(g)



675

676

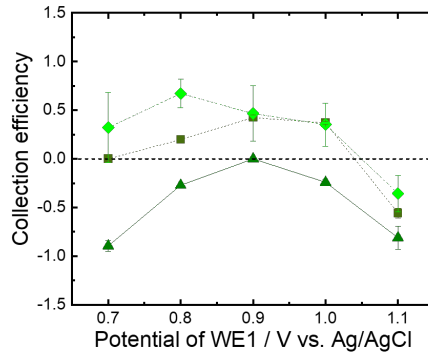
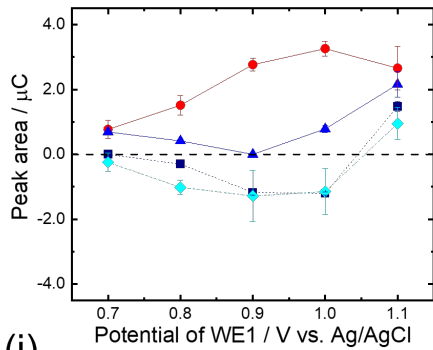
677

678

679 **Fig. 3.** Continued.

680

(h)



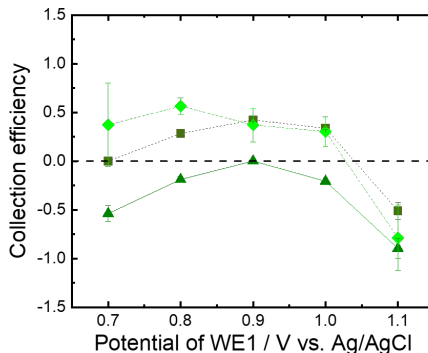
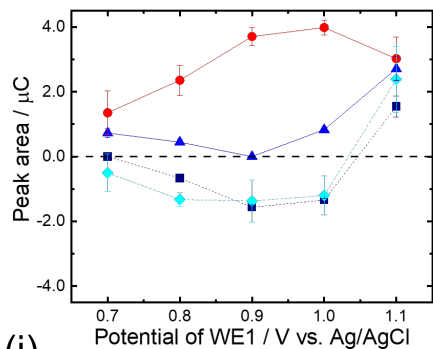
681

682

683

684

(i)



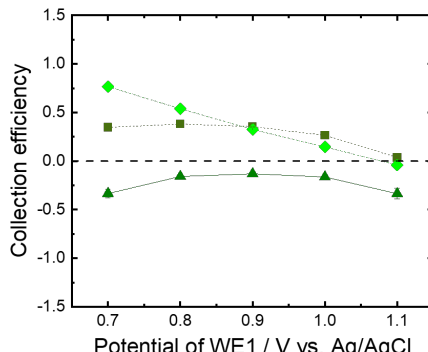
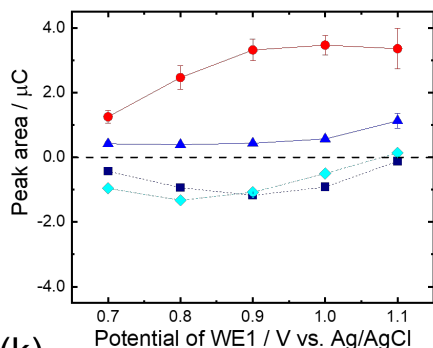
685

686

687

688

(j)



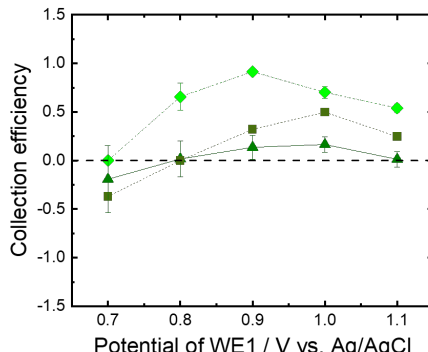
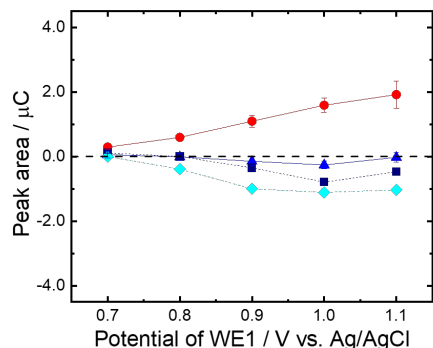
689

690

691

692

(k)



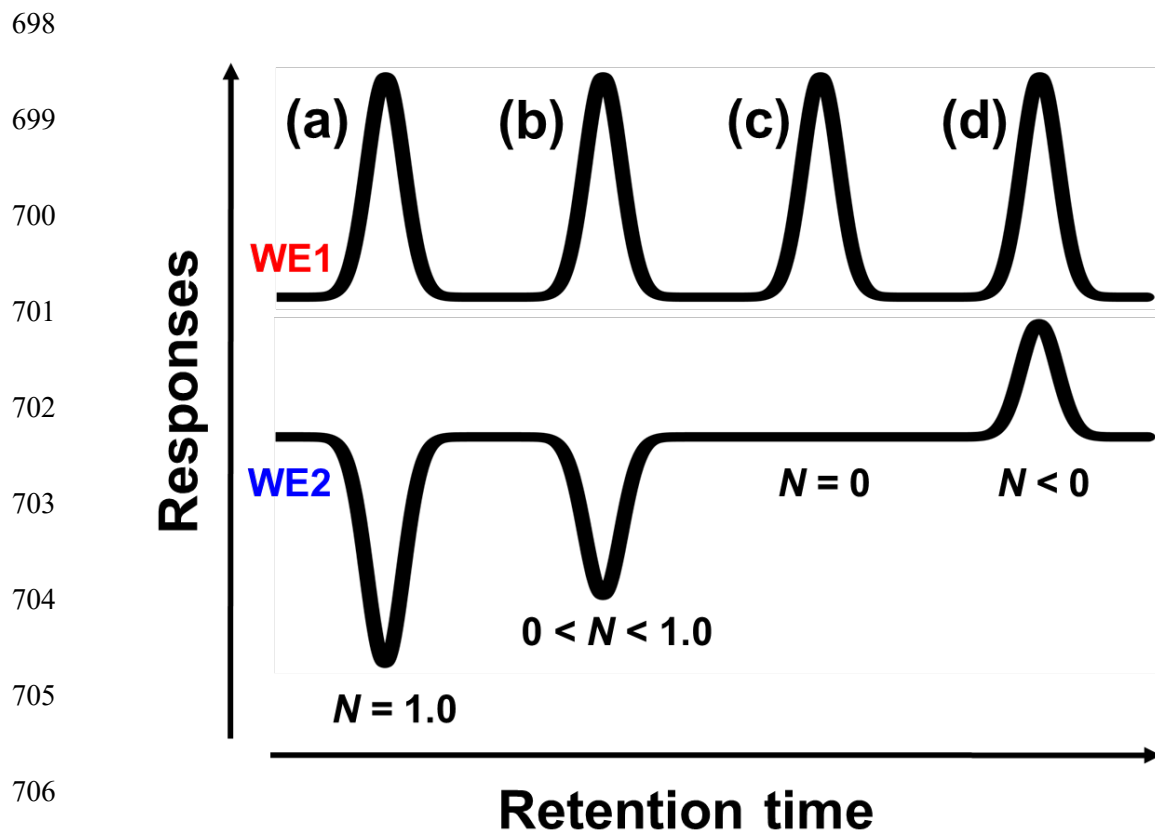
693

694

695

696

697 **Fig. 3.** Continued.

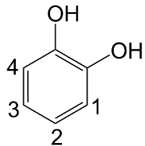
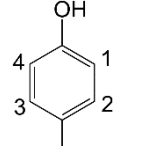
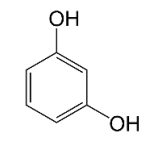
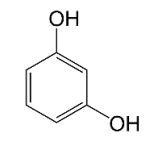
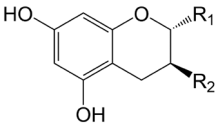
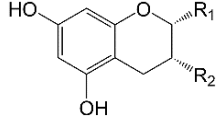
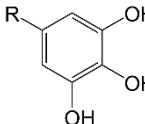


709 **Fig. 4.** The detection patterns of the 11 phenolic compounds obtained with the proposed
 710 dual-electrode. Collection efficiencies reflect the molecular structures and
 711 electrochemical reversibility, and vary over a broad range from negative values to 1.0.

712
 713
 714
 715

716 **Table 1** Details for the 11 phenolic compounds.

717

No.	Compounds	Substituent	Structure
1	catechol	1,2,3,4-H	
2	protocatechuic acid	1,3,4-H, 2-COOH	
3	caffeic acid	1,3,4-H, 2-CH=CH-COOH	
4	chlorogenic acid (3-CQA)	1,3,4-H, 2-CH=CH-COO-R, R = quinic acid	
5	hydroquinone	1,2,3,4-H	
6	gentisic acid	1-COOH, 2,3,4-H	
7	resorcinol		
8	(+) - catechin	R ₁ = catechol, R ₂ = OH	
9	(-) - epicatechin	R ₁ = catechol, R ₂ = OH	
10	pyrogallol	R = H	
11	gallic acid	R = COOH	

718

719